

MODELLING EXTREME SEA LEVELS DUE TO SEA LEVEL RISE AND STORM SURGE IN THE SETO INLAND SEA, JAPAN

Han Soo Lee^{1, 2}

The extreme sea level due to storm surge and future sea-level rise (SLR) in the year of 2050 and 2100 are estimated by using ensemble empirical mode decomposition (EEMD) and extreme value analysis (EVA) with long-term sea level records in and around the Seto Inland Sea, Japan. Ensemble empirical mode decomposition, an adaptive data analysis method, can separate the tidal motions and the non-linear trend from the sea level records to reconstruct the storm surge levels, and then the reconstructed storm surge levels are applied to statistical model, EVA, to obtain the extreme storm surges at 95% confidence interval in the target return periods. The SLR trend at Tokuyama in the Seto Inland Sea obtained from EEMD is 3.58 mm/yr over 1993-2010, which is slightly larger than the recent altimetry-based global rate of 3.3 ± 0.4 mm/yr over 1993-2007. The resulting SLR in 2050 and 2100 estimated are 0.18 m and 0.49 m, respectively. The 30-, 50-, and 100-yr return levels at Tokuyama obtained by EVA are 1.30 m, 1.43 m and 1.64 m. Therefore, the extreme sea level in 2050 and 2100 due to future SLR and storm surge with 100-yr return level would be 1.82 m (1.35 m ~ 2.26 m with 95% confidence intervals) and 2.13 m (1.75 m ~ 3.10 m with 95% confidence intervals), respectively. The SLR is not only due to mass and volume changes of sea water, but also due to other factors such as local subsidence, river discharge and sediments, and vegetation effect. The non-linear trend of SLR, which is the residue from EEMD, can be regarded as a final consequential sea level after considering those factors and their nonlinearity. The combined EEMD-EVA method can be useful tool not only for the extreme sea level estimation under climate change, but also for many cases in coastal engineering and hydrology.

Keywords: extreme sea level; sea level rise; storm surge; ensemble empirical mode decomposition; extreme value analysis; the Seto Inland Sea

INTRODUCTION

Recently, it is commonly accepted that global mean sea levels have increased steadily over the past century as a result of an increase of the global mean atmospheric temperature (Cazenave and Llovel, 2009; IPCC, 2007). Continued increases in mean sea levels are predicted to have catastrophic impacts on coastal environments around the world in the coming near future. Coastal hazards due to flood events are almost invariably associated with extreme sea levels by tropical cyclone induced storm surges (Butler et al., 2007a). Therefore, the impacts of global warming on coastal flood risk depend heavily on the extreme surge trend in the future.

According to Flather (2001), the storm surges are transient distortions in the sea surface level which result from storm-induced winds and atmospheric pressure. In a recent study, the surface waves through wave breaking in shallow water also play critical role in amplifying storm surge levels due to tropical cyclone (Lee et al., 2013). The storm surge levels can be “positive” and “negative” in elevation and be derived by removing the predicted astronomical tide level from the observed sea surface level. Extreme positive storm surges, thus, are the major factor in coastal flooding along the shoreline with shallow water and low-lying coastal environment. The future projection of extreme positive storm surge, thus, is crucial in the coastal defense under the climate change impacts and adaptation strategies.

In climate change impact studies on coastal flooding, for example, in Bangladesh which is one of the most vulnerable countries to SLR and storm surge (Ali, 1996; 1999; Karim and Mimura, 2008; Rahman, 2009; Ruane et al., 2013; Sarwar, 2005), the SLR projections are adapted by simple scenarios, for instance 1 m rise by 2100, or by physical process-based dynamic (deterministic) modeling approaches, for example a (ensemble) simulation result from the global climate models (GCMs) with high uncertainty. Moreover, storm surge is not usually or explicitly considered in the scenarios. On the other hands, in the coastal defense against extreme storm surges using deterministic hydrodynamic modeling approaches (2013a; Haigh et al., 2013b) or statistical modeling approaches (Butler et al., 2007a; 2007b; 2013a; Haigh et al., 2013b), the impact of SLR is not usually and explicitly considered, either. Lee (2013) recently reported a novel way to explicitly estimate the regional extreme sea levels due to both sea level rise and storm surge in Bangladesh, and showed further projection for regional scenarios of extreme sea levels.

¹ Graduate School of Science and Engineering, Saitama University, 255 Shimo-okubo, Sakura-ku, Saitama, Saitama 338-8570, Japan

² International Institute for Resilient Society, Saitama University, Saitama, Japan

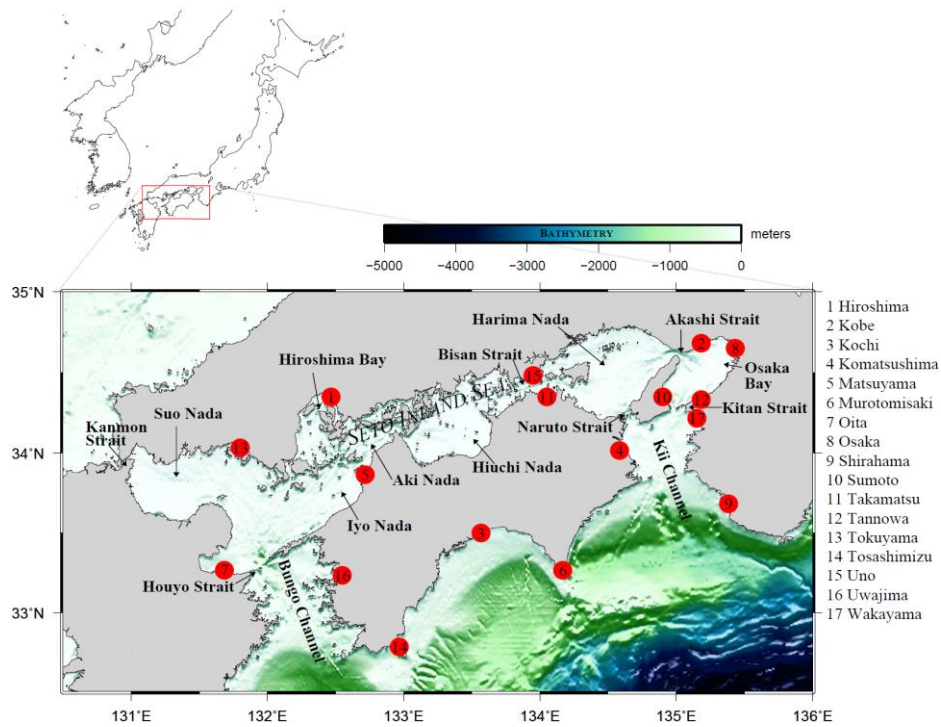


Figure 1. Tidal stations for sea level records in and around the Seto Inland Sea (SIS). Nada in Japanese means basin.

The Seto Inland Sea (SIS) is a largest long channel-shaped enclosed coastal sea in the western part of Japan with a size of about 23,000 km², a length of about 500 km and an average depth of about 38 m (Tsuge and Washida, 2003; Yamamoto, 2003; Yanagi et al., 1982). It is connected to the outer Pacific Ocean and sea via the Kii Channel, the Bunge Channel and the Kamon Strait. In addition to its mild climate and beautiful scenery of sandy beaches, tidal flats, and historical heritages, it includes approximately 1000 islands and a number of narrow waterways/straits (Seto in Japanese) connecting the basins (Nada in Japanese) and bays (Fig. 1). As parts of Japanese coast under frequent passes of typhoons in summer, the SIS experiences frequent storm surges (Lee et al., 2010).

In this study, we estimate the extreme sea level due to (1) storm surge and (2) future SLR based on data-driven statistical modeling approach using ensemble empirical mode decomposition (EEMD) and extreme value analysis (EVA) with long-term sea level records in and around the SIS, Japan, as illustrated in Lee (2013). We demonstrate regional projection of extreme sea level (=extreme positive storm surges + SLR) to the mid- and long-term future by the years of 2050 and 2100.

DATA AND METHOD

Data

The observed sea levels from 17 stations in and around the Seto Inland Sea, Japan, are obtained from Japan Meteorological Agency (JMA) and Japan Coastal Guard (JCG). The observed data periods used in this study are all different for each station. The longest hourly dataset used comprises for 61 years from January 1 1950 to December 31 2010 at Tokuyama, the Station No. 13 in Fig. 1. The total number of original raw data at Tokuyama is 534,720 with intermittent missing data of total 10,915 (2.04% of complete data). The other stations also show missing data fractions less than 10% of complete data except the Kochi station with 13.34%. The observed tidal levels at all stations are referenced with respect to the Tokyo Peil (TP) of Japan. In the analyses, the predicted tides for the missing data are adjusted after reflecting the relationship between the datum and TP at each station (Table 1). Since the Tokuyama station gives the longest information on sea level change, we demonstrate the detailed data analysis procedure for estimating the future extreme sea level hereinafter with the sea level records from the Tokuyama station. Table 1 shows the details of the observations at 17 stations including the locations, the available periods, the percent of missing data, and the datum.

No.	Station	Location		Data period	Missing (%)	Interval (hr)	Datum (TP, Unit: cm)
		Lat (E)	Long (N)				
1	Hiroshima	34°21'	132°28'	Jan. 1952-Dec. 2010	4.10	1	-308.0
2	Kobe	34°41'	135°11'	Jan. 1965-Dec. 2009	2.30	1	-168.2
3	Kochi	33°30'	133°34'	Jan. 1968-Dec. 2009	13.34	1	-95.4
4	Komatsushima	34°1'	134°35'	Jan. 1964-Dec. 2009	5.54	1	-191
5	Matsuyama	33°52'	132°43'	Jan. 1961-Dec. 2009	2.21	1	-214.7
6	Murotomisaki	33°16'	134°10'	Jan. 1967-Dec. 2009	7.24	1	-292.6
7	Oita	33°16'	131°41'	Jan. 1967-Dec. 2010	2.03	1	-309.5
8	Osaka	34°39'	135°26'	Jan. 1961-Dec. 2009	2.11	1	-353.7
9	Shirahama	33°41'	135°23'	Jan. 1968-Dec. 2009	1.41	1	-314.2
10	Sumoto	34°21'	134°54'	Jan. 1965-Dec. 2009	1.31	1	-184.5
11	Takamatsu	34°21'	134°3'	Jan. 1965-Dec. 2009	1.31	1	-189.8
12	Tannowa	34°20'	135°11'	Jan. 1967-Dec. 2009	3.91	1	-173
13	Tokuyama	34°2'	131°48'	Jan. 1950-Dec. 2010	2.04	1	-256.3
14	Tosashimizu	32°47'	132°58'	Jan. 1961-Dec. 2009	0.2	1	-156.1
15	Uno	34°29'	133°57'	Jan. 1965-Dec. 2009	5.69	1	-171.6
16	Uwajima	33°14'	132°33'	Jan. 1964-Dec. 2009	5.26	1	-207.8
17	Wakayama	34°13'	135°9'	Jan. 1967-Dec. 2009	2.54	1	-94.3

Trend and detrending

In the data analysis, finding a trend and removing the trend found is one of most basic and important steps. However, there is neither precise definition of “trend” nor any logical algorithm for detrending it. As a result, there are various ad hoc extrinsic methods available for determining trend and detrending it, such as from the most common straight line best fit based on simple linear trend to a moving average method. Such a simple trend is suit for linear and stationary data, and the moving average method requires a predetermined time scale which is unknown *a priori* for nonstationary processes. In general curve-fitting and filtering methods, data fits to predetermined parametric functions which are subjective often based on assumptions of stationarity and linearity. Sea level changes are non-stationary and non-linear natural processes in which the underlying physical processes and their non-linear interactions affecting sea levels are not completely known.

Based on Wu et al. (2007), we define the trend and detrending as follows.

The *trend* is an intrinsically fitted monotonic function or a function in which there can be at most one extremum with a given data span. *Detrending* is the operation of removing the trend. The variability is the residue of the data after the removal of the trend within a given data span. The given data span in the trend definition could be a part or the whole length of the data used.

Based on the definition of trend above, we determined the whole length of dataset used as for the data span. Therefore, the residue is selected as the non-linear trend representing a local property of the data, which is the overall trend of SLR within the whole data span at each station.

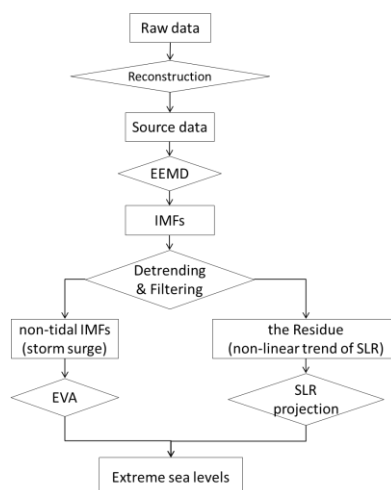


Figure 2. Data analysis procedure for modeling the extreme sea level due to storm surge and sea level rise using EEMD and EVA.

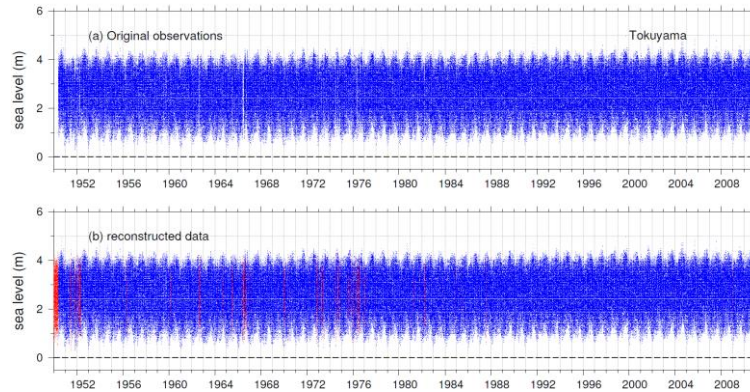


Figure 3. (a) Original observed raw data at Tokuyama and (b) the reconstructed source data after filling in the missing gaps with supplementary predicted data using a high-resolution tide model.

Empirical Mode Decomposition

In contrast to the general curve-fitting and filtering methods, empirical mode decomposition (EMD) method is empirical, intuitive, direct, and adaptive, without requiring any predetermined parametric functions for determining trend and detrending (Huang et al., 1999; Huang et al., 1998). Therefore, it suits for the purpose of finding out the intrinsic monotonic function for trend and detrending from nonstationary and nonlinear dataset.

The decomposition is based on the simple assumption that any data consists of different simple intrinsic modes of oscillations. This method is also based on the direct extraction of energy associated with various intrinsic time scales. Each of these oscillatory modes is represented by an intrinsic mode function (IMF) while satisfying the following conditions: (1) in the whole data set, the number of extrema and the number of zero-crossings must either be equal or differ by, at most, one; and (2) at any point, the mean value of the envelope defined by the local maxima and the envelope defined by the local minima is zero. The IMF can have both variable amplitude and frequency as functions of time, whereas the simple harmonic function has constant amplitude and frequency. IMFs with periods that are too long relative to the data length to be separated by spectral analysis methods can still be identified and decomposed by the EMD.

The EMD decomposes an arbitrary data set $x(t)$, in terms of IMFs, $C_j(t)$, and a residue, $R_n(t)$, through a “sifting process”, where $j = 1, 2, 3, \dots, n$. Therefore, the original data $x(t)$ can be reconstructed by adding up all modes and the residue, $x(t) = C_1(t) + C_2(t) + C_3(t) + \dots + R_n(t)$. The $R_n(t)$ could be a simple constant or a monotonic functions from which no more oscillatory IMFs can be extracted. In the case of sea level records analysis, it is the trend of SLR.

Ensemble empirical mode decomposition (EEMD) is the improved method for obtaining IMFs with more direct physical meaning and greater uniqueness (Wu and Huang, 2009). The EEMD defines the true IMF components as the mean of an ensemble of trials, which consist of the time series plus the white noise of finite amplitude. This method dramatically improves the mod mixing problem due to the subject selection of scale in scale separation. The EEMD method was applied in this study to analyse the sea level records. The EEMD were tested with respect to the optimum number of ensemble in EEMD analysis. The result showed that ensemble number larger than 20 gives a robust result in terms of the statistical significance of resulting IMFs. Therefore, the number of ensemble was set to 30 for all analyses with the standard deviation of 0.2. Consequently, to determine whether a dataset or its components contain useful information, statistical significance tests were performed based on the characteristics of Gaussian white noise with EEMD. The results of EEMD of the sea level records in the SIS showed that all IMFs are statistically significant at the 95% and 99% confidence-limit levels.

Parameter	Estimate	Std. error
Location (μ)	0.669	0.021
Scale (σ)	0.133	0.017
Shape (ξ)	0.185	0.139

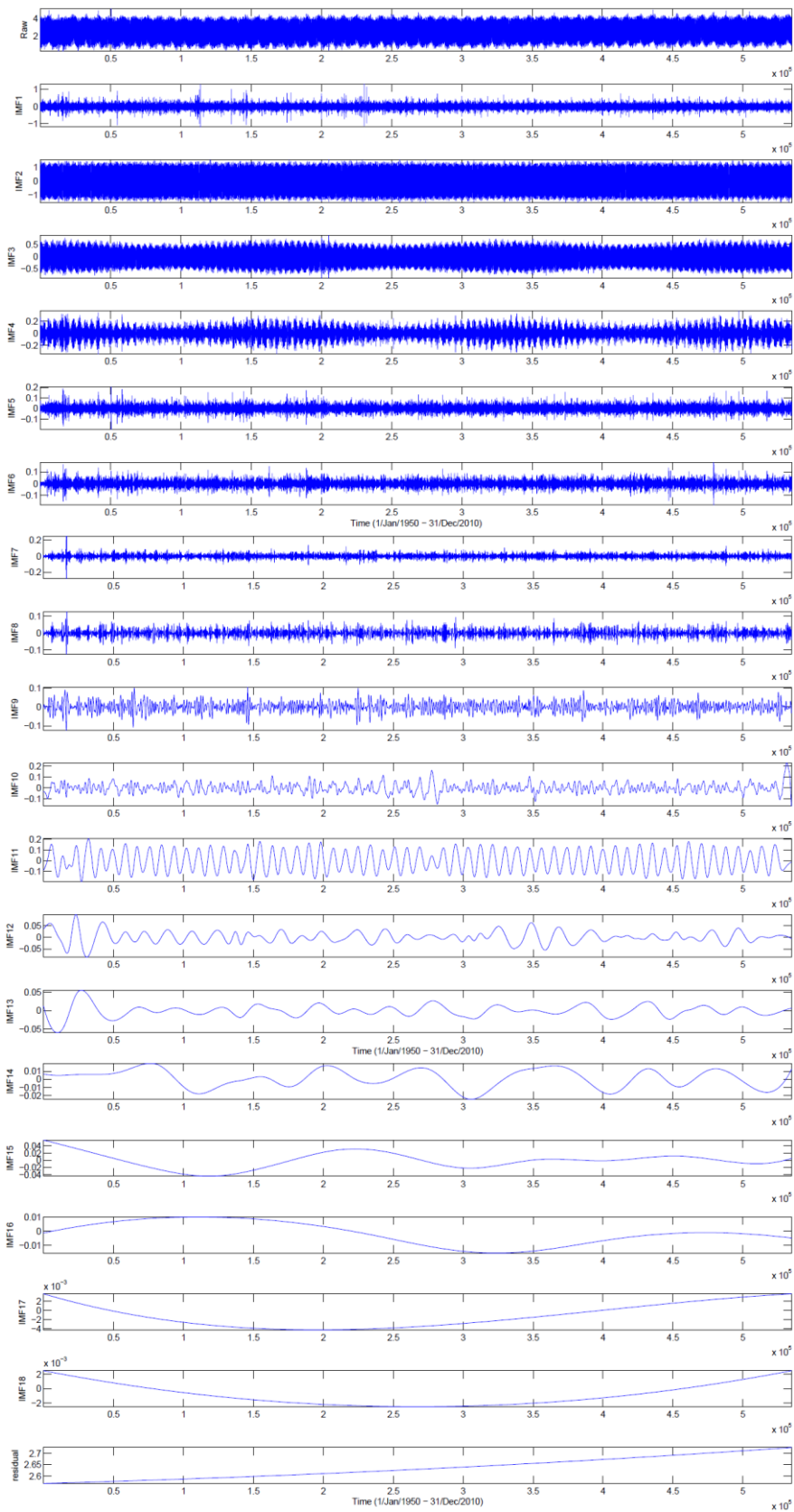


Figure 4. The reconstructed source data (Raw), IMFs and the residual obtained by EEMD at Tokuyama.

Extreme value theory

The distinguish feature of an EVA is the objective to quantify the stochastic behaviour of a process at unusually large or small levels. In particular, EVA usually requires estimation of the probability of events that are more extreme than any ever observed and is a widely-used statistical methodology (Coles, 2001). In extreme storm surge study, Butler et al. (2007a; 2007b) exhibits good applications of EVA to storm surge levels in the North Sea.

For the n years of hourly surge data, s_1, \dots, s_n , and let z_j denote the annual maximum surge for year s_j . A standard procedure is to assume that the annual maxima z_1, \dots, z_n follow a general extreme value (GEV) distribution with the form

$$G(z; \theta) = \exp \left[- \left\{ 1 + \xi \left(\frac{z - \mu}{\sigma} \right) \right\}^{-\frac{1}{\xi}} \right] \quad (1)$$

where $\theta = (\mu, \sigma > 0, \xi)$ are location, scale and shape parameters respectively. Positive values of the shape parameter ($\xi > 0$) correspond to heavy-tailed while negative values ($\xi < 0$) mean light-tailed distributions. The uniform distribution ($\xi = -1$) and $\xi = 0$ (the Gumbel distribution) arises when the upper tail decays exponentially.

The parameters can be estimated by maximum likelihood method and thereby more easily interpretable quantities, in particular, the T -year return level (or design values) in hydrology and coastal engineering can be estimated in the following form

$$q(T) = \mu - \frac{\sigma}{\xi} \left[1 - \left\{ -\log \left(\frac{T-1}{T} \right) \right\}^{-\xi} \right] \quad (1)$$

which correspond to the level that is exceeded with probability $1/T$ in any particular year.

Extreme value analysis typically adapts one of two alternative approaches by modelling either the exceedances of a high threshold or the maxima of data blocks, block maxima. In this study, we use the block maxima to estimate the return levels of storm surges in and around the SIS for potential extreme storm surge. The confidence interval for the return level is obtained based on the delta method, which assumes normality for the return levels. The delta method is a general approach for computing confidence intervals for functions of maximum likelihood estimates. The delta method takes a function that is too complex for analytically computing the variance, creates a linear approximation of that function, and then computes the variance of the simpler linear function that can be used for large sample inference (Coles, 2001; Xu and Long, 2005).

For this study, the Extremes Toolkit (extRemes) (Gilleland and Katz, 2005; 2011), operated through the open-source 'R' software, is used to apply the extreme value analysis method to estimate return periods and return levels of storm surge.

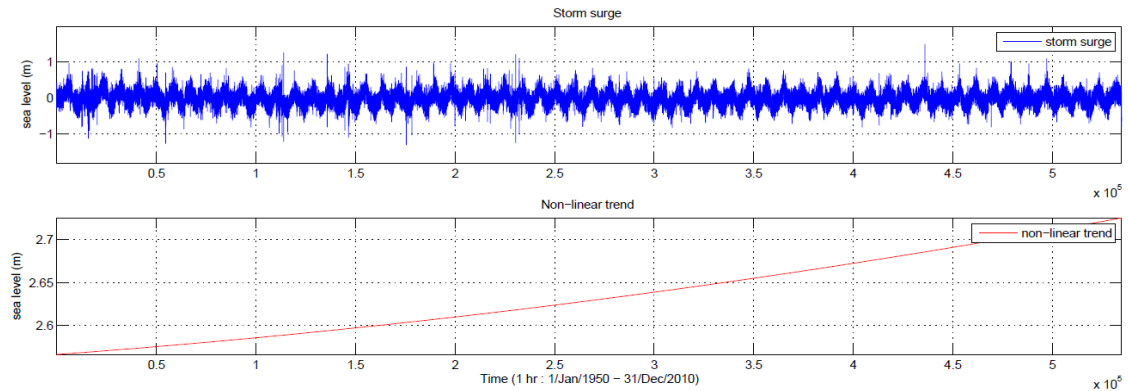


Figure 5. The reconstructed storm surges (blue) from the non-tidal IMFs and the non-linear trend (red) from the residual at Tokuyama.

Analysis procedure

Figure 2 depicts the procedure of data analysis and statistical modelling for estimating the extreme sea level using EEMD and EVA.

First, since the observed records at Tokuyama contain intermittent missing data, a reconstruction of data is carried out by filling in the missing data with supplementary predicted tides generated using NAO99 global tide model (Matsumoto et al., 2000). Figure 3 illustrates (a) the original raw data and (b) the reconstructed source data with the predicted tides in red.

Second, the reconstructed source data is applied to EEMD with 30 ensembles. The EEMD produces 18 IMFs from high to low frequencies and the residual from the source data (Fig. 4). The statistical significant test is, then, performed to ensure the significance levels of all IMFs. The result shows that all IMFs are statistically significant at 99% confidence limit.

Third, after ensuring the significance levels of IMFs, the residual is removed from the EEMD results for detrending the reconstructed source data. Then, the IMFs correspond to astronomical tidal components are eliminated from the EEMD results. Therefore, the storm surge levels could be reconstructed by combining the remained non-tidal IMFs (Fig. 5(a)). The EEMD is used as a tool for detrending and filtering method in this process. In other words, by applying the EEMD, we can detrend the source data and filter out tidal components concurrently and automatically for the EVA of storm surge in the next process.

Fourth, we calculate the annual maxima from the reconstructed storm surge levels obtained in the previous process. Then, apply them to the EVA using block maxima and fitting to GEV distribution to estimate the return levels of storm surge for target years with confidence intervals (Fig. 6).

Fifth, for future projection of sea level rise, we use the above-mentioned residue from the EEMD results as the non-linear trend of sea level change (Fig. 5(b)). In addition to the volume and mass changes of sea water, there are many other factors contributing to sea level change such as river discharge, sediments, and land subsidence (Miller and Douglas, 2004). We interpret that the non-linear trend represents the sea level change resulting from the non-linear interaction among those factors. To project of future SLR, we use the current non-linear trend of the reconstructed source data. We tried various functions and selected a quadratic polynomial, which fits exactly the non-linear trend of sea level change ($r=1.0$). Then, the polynomial function is extended straightforward to predict the sea level change to 2100 (Fig. 7(a)). Therefore, the current acceleration of the sea level rise in the non-linear trend is taken into account in the future prediction.

Finally, by combining the estimated return level and projected SLR for a target year, we can obtain the extreme sea level due to SLR and storm surge quantitatively with confidence levels (see Fig. 7).

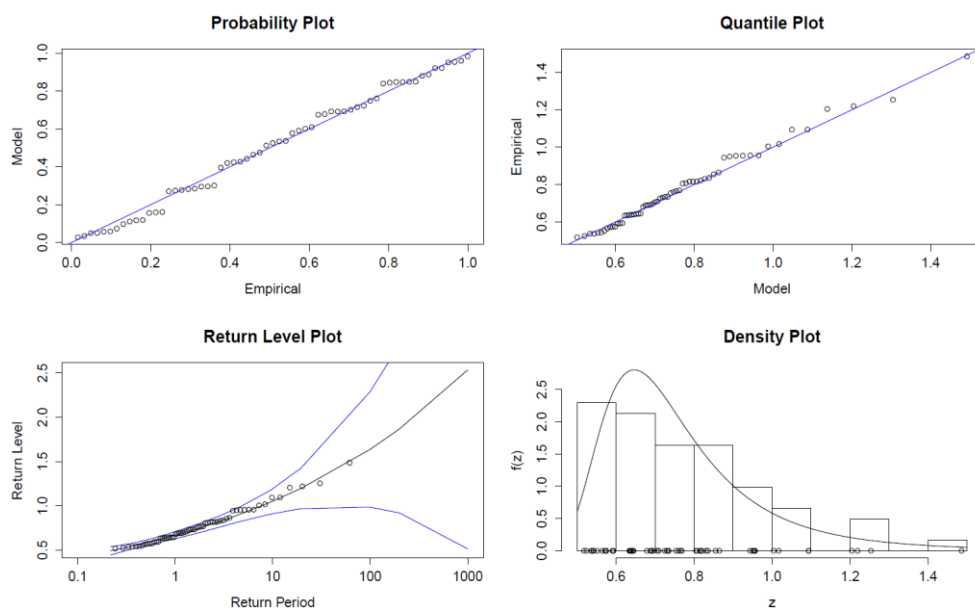


Figure 6. Diagnostic results from the extreme value analysis for the annual maxima of storm surges. (a) Probability plot, (b) Q-Q plot, (c) Return level plot and (d) Density plot.

RESULTS

Storm surge from EEMD

IMFs of the sea level records at Tokuyama, decomposed using the EEMD method described above, are shown in Fig. 4. The figure depicts that IMF1 is composed of the finest timescales, or highest frequency, and the timescale increases as the index j of IMF $_j$ increases. Interestingly, the result of statistical significance test showed that all IMFs are statistically significant at the 99% confidence level.

As can be noted, the IMF2 and IMF3 correspond to the composites of semi-diurnal and diurnal tides, respectively. Due to its adaptive nature of EEMD method, it is possible to interpret that the semi-diurnal tides such as M_2 , S_2 , N_2 , and K_2 are embedded in the IMF2. Analogous to the case of IMF2, the IMF3 can represent the mixed signal of diurnal tides such as K_1 , O_1 , P_1 , and S_1 . IMF11 indicates the clear seasonal cycle due to annual tendency of the context of East Asian monsoon in the sea level. Those three IMF 2, 3, and 11 depict the highest normalized energy density in the signal based on the result of significance test.

The highest frequency IMF1 can be interpreted as a sea level response to weather, termed as weather cycle in Tebaldi et al. (2012). In the Pacific Ocean, the El Niño and La Niña episodes have irregular intervals for their occurrence of 3-5 years (in the historical record, this interval varies from 2 to 7 years) (Lee et al., 2012). Since the oscillatory IMFs contain possible physical meanings, the IMF12, IMF13 and IMF14 may correspond to the irregular occurrence intervals of the El Niño and La Niña episodes. IMF7, IMF8 and IMF10 may correspond to the lunar fortnightly tide, M_f , the lunar monthly tide, M_m , and the solar semi-annual tide, S_{as} , based on their mean periods. They are the examples of how the IMFs can be interpreted. However, due to our limited knowledge on physical phenomena causing the sea level responses, it is still challenging and needs various and thorough case studies to find out the physical meanings for each IMF depending on one's objectives.

Upon the purpose of this study to estimate the extreme storm surge using the EVA in the next step, we reconstruct the storm surge levels by combining all non-tidal IMFs after only removing the IMF2 and IMF3 and the residual, corresponding to composites of semi-diurnal and diurnal tides and the non-linear trend, respectively, as indicated above. In Fig. 5, the reconstructed storm surge levels are presented with blue lines together with the residue, the non-linear trend, in red.

Storm surge return levels from EVA

A maximum value for each year is calculated from the reconstructed storm surge levels. Then, the annual maxima ($n = 61$) obtained from the reconstructed storm surge levels for the 61-year (1950 ~ 2010) at Tokuyama are applied to the EVA, and the results such as the probability plot, the Quantile-Quantile (Q-Q) plot, the return level plot and the density plot are presented in Fig. 6. The Q-Q plot is widely used diagnostic tool for comparing the distributional properties of a fitted statistical model against the empirical distribution of data. The blue lines in the probability plot and the Q-Q plot indicate the perfect fit of a statistical model. The blue lines in the return level plot represent the 95% confidence interval. The distribution parameters by the maximum likelihood estimation are given in Table 2. The 100-yr return level at Tokuyama is 1.64 m with 95% confidence interval, 1.26 ~ 2.61 m (Fig. 7(b)). The detailed return levels for all stations are presented in Table 3.

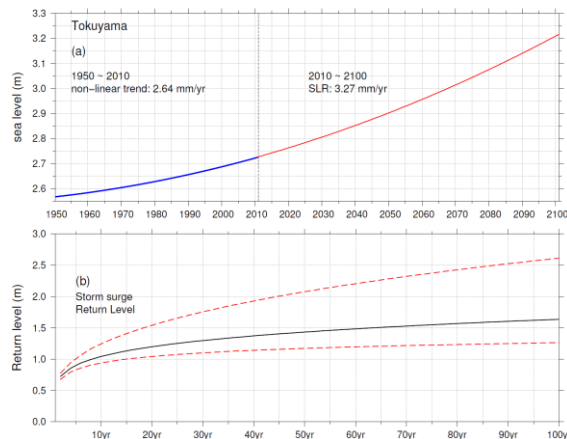


Figure 6. Diagnostic results from the extreme value analysis for the annual maxima of storm surges. (a) Probability plot, (b) Q-Q plot, (c) Return level plot and (d) Density plot.

Sea level rise projection

As a result of EEMD method, the residue is obtained together with IMFs. As described earlier, we interpret the residue as the non-linear trend of sea level records. The red line in Fig. 5 indicates the non-linear SLR trend. The annual rates of sea level changes at Tokuyama are 2.64 mm/yr for 1950 ~ 2010 and 3.58 mm/yr for 1993 ~ 2010 which is slightly larger than the altimetry-based global average SLR rate of 3.3 ± 0.4 mm/yr from 1993-2007 (Cazenave and Llovel, 2009). To predict the future SLR to 2100, the non-linear trend is fitted to a quadratic polynomial ($r=1.0$). Then, the polynomial is extended to the year of 2100 for SLR projection taking into account the current acceleration trend of SLR. The resulting SLR from 2010 to December 2100 is 0.49 m with average annual rate of 3.27 mm/yr (See Table 3 and Fig. 7(a)).

CONCLUSIONS

We have introduced a novel approach to estimate the extreme storm surge and future SLR by combining an adaptive data analysis method, EEMD, and a statistical modeling method, EVA, using a long-term observed sea level records at Tokuyama in SIS, Japan.

The EEMD method successfully filters out the tidal variations in the raw sea level records to reconstruct storm surge levels. The non-linear SLR trend could also be identified and obtained from the residual from EEMD. The annual mean rates of SLR at Tokuyama obtained are 2.64 mm/yr from 1950 to March 2010 and 3.58 mm/yr from April 1993 to March 2010, which is slightly larger than the altimetry-based rate of global average SLR of 3.3 ± 0.4 mm/yr over 1993-2007. The SLR projection in 2050 and in 2100 obtained are 0.18 m and 0.49 m, respectively. Then, the reconstructed storm surge elevations undergo the EVA to estimate the extreme storm surges at Tokuyama. The obtained 30-, 50-, and 100-yr return levels are 1.3 m, 1.43 m and 1.64 m, respectively. Therefore, the extreme sea level in 2100 due to future SLR and storm surge with 100-yr return level would be 2.13 m with 95% confidence interval, 1.75 m ~ 3.10 m.

Coastal floods associated with storm surges are the world's foremost natural hazard, surpassing even earthquakes for loss of life and property damage (Shah, 1983). With respect to the TC activity in the future, there is a growing concern and consensus for an increase of TC intensity and frequency due to global warming (Trenberth et al., 2007). In many reported adaptation strategies to future SLR, for example, in Bangladesh which is one of the most vulnerable countries to SLR and storm surge, the storm surge levels are usually or explicitly not considered in simple SLR scenarios with high uncertainty. In adaption strategies to climate change, however, the SLR scenarios due to storm surge and global warming, and its estimation are not trivial and have to be estimated physically and statistically sound. In coastal engineering point of view, the information from both storm surges and SLR is a critical factor in coastal defense for future climate change. Therefore, we hope the introduced novel method using EEMD and EVA would help improve the procedures of assessments and adaptations to climate change and in coastal defense.

Table 3. Distribution parameters estimated by maximum likelihood for Tokuyama station.

No	Station	Trend (mm/yr)		Sea level rise (m)		Return level (m)		
		Available period	1993~	2050	2100	30-yr	50-yr	100-yr
1	Hiroshima	+4.44	+5.18	+0.20	+0.46	1.17	1.22	1.29
2	Kobe	+8.23	+17.71	+1.46	+4.72	0.99	1.03	1.07
3	Kochi	+0.78	+6.17	+0.74	+2.61	1.38	1.48	1.61
4	Komatsushima	+1.55	+1.27	+0.02	+0.00	1.13	1.15	1.18
5	Matsuyama	+0.77	+0.22	-0.03	-0.15	1.44	1.57	1.76
6	Murotomisaki	+5.11	+7.01	+0.43	+1.25	1.22	1.26	1.32
7	Oita	+3.30	+2.47	+0.01	-0.13	0.90	0.93	0.96
8	Osaka	+10.25	+3.82	-0.35	-1.72	1.08	1.15	1.24
9	Shirahama	-0.93	+0.06	+0.11	+0.44	0.72	0.74	0.77
10	Sumoto	+2.48	+2.69	+0.12	+0.28	0.82	0.86	0.90
11	Takamatsu	+1.87	+1.21	-0.01	-0.15	1.18	1.25	1.36
12	Tannowa	+1.54	+1.52	+0.05	+0.10	0.78	0.80	0.82
13	Tokuyama	+2.64	+3.58	+0.18	+0.49	1.30	1.43	1.64
14	Tosashimizu	+1.03	+2.02	+0.15	+0.46	0.77	0.79	0.80
15	Uno	+5.00	+3.84	+0.04	-0.13	1.25	1.37	1.55
16	Uwajima	+0.68	+1.05	+0.07	+0.21	1.26	1.28	1.30
17	Wakayama	-0.76	-0.48	+0.01	+0.07	0.82	0.85	0.89

With respect to the SLR projection, a semi-empirical approach was suggested to project SLR by connecting global SLR to global mean surface temperature (Rahmstorf, 2007; Tebaldi et al., 2012; Vermeer and Rahmstorf, 2009). They showed that the semi-empirical formula hold to good approximation for temperature and sea level changes during the 20th century. In a future work, we improve the SLR projection by comparing and applying the semi-empirical formula rather than simply expanding a polynomial to future.

ACKNOWLEDGMENTS

This study is supported by the Grant-in-Aid for Young Scientists (B) and the Grant-in-Aid for Challenging Exploratory Research of MEXT.

REFERENCES

- Ali, A. 1996. Vulnerability of Bangladesh to climate change and sea level rise through tropical cyclones and storm surges, *Water, Air, & Soil Pollution*, 92(1), 171-179.
- Ali, A. 1999. Climate change impacts and adaptation assessment in Bangladesh, *Climate Research*, 12(2-3), 109-116.
- Butler, A., J. E. Heffernan, J. A. Tawn, and R. A. Flather. 2007a. Trend estimation in extremes of synthetic North Sea surges, *J. R. Stat. Soc.*, 56(4), 395-414.
- Butler, A., J. E. Heffernan, J. A. Tawn, R. A. Flather, and K. J. Horsburgh. 2007b. Extreme value analysis of decadal variations in storm surge elevations, *J. Mar. Syst.*, 67(1-2), 189-200.
- Cazenave, A., and W. Llovel. 2009. Contemporary Sea Level Rise, *Annual Review of Marine Science*, 2(1), 145-173.
- Coles, S. 2001. *An introduction to statistical modeling of extreme values*, 208 pp., Springer-Verlag, London, UK.
- Flather, R. A. 2001. Storm Surges, in *Encyclopedia of Ocean Sciences*, edited by H. S. John, pp. 2882-2892, Academic Press, Oxford.
- Gilleland, E., and R. W. Katz. 2005. Extreme Toolkit (extRemes): Weather and Climate Applications of Extreme Value Statistics, *Rep.*, 130 pp, NCAR, Research Applications Laboratory (RAL), Boulder, CO, U.S.A.
- Gilleland, E., and R. W. Katz. 2011. New software to analyze how extremes change over time, *EOS TRANS. AGU*, 92(2).
- Haigh, I., E. M. S. Wijeratne, L. MacPherson, C. Pattiaratchi, M. Mason, R. Crompton, and S. George. 2013a. Estimating present day extreme water level exceedance probabilities around the coastline of Australia: tides, extra-tropical storm surges and mean sea level, *Climate Dynamics*, 1-18.
- Haigh, I., L. MacPherson, M. Mason, E. M. S. Wijeratne, C. Pattiaratchi, R. Crompton, and S. George. 2013b. Estimating present day extreme water level exceedance probabilities around the coastline of Australia: tropical cyclone-induced storm surges, *Climate Dynamics*, 1-19.
- Huang, N. E., Z. Shen, and S. R. Long. 1999. A new view of nonlinear water waves: The Hilbert spectrum, *Annu. Rev. Fluid Mech.*, 31(1), 417-457.
- Huang, N. E., Z. Shen, S. R. Long, M. C. Wu, H. H. Shih, Q. Zheng, N. C. Yen, C. C. Tung, and H. H. Liu. 1998. The empirical mode decomposition and the Hilbert spectrum for nonlinear and non-stationary time series analysis, *Proc. R. Soc. London.*, 454(1971), 903-995.
- IPCC 2007. *Climate Change 2007: The Physical Science Basis*. Contribution of Working Group I to the Fourth Assessment Report of the Intergovernmental Panel on Climate Change, edited by S. Solomon, D. Qin, M. Manning, Z. Chen, M. Marquis, K. B. Averyt, M. Tignor and H. L. Miller, Cambridge University Press Cambridge, United Kingdom and New York, NY, USA.
- Karim, M. F., and N. Mimura. 2008. Impacts of climate change and sea-level rise on cyclonic storm surge floods in Bangladesh, *Global Environ. Change*, 18(3), 490-500.
- Lee, H. S. 2013. Estimation of extreme sea levels along the Bangladesh coast due to storm surge and sea level rise using EEMD and EVA, *Journal of Geophysical Research: Oceans*, 118(9), 4273-4285.
- Lee, H. S., T. Yamashita, and T. Mishima. 2012. Multi-decadal variations of ENSO, the Pacific Decadal Oscillation and tropical cyclones in the western North Pacific, *Progress In Oceanography*, 105(0), 67-80.

- Lee, H. S., T. Yamashita, T. Komaguchi, and T. Mishita. 2010. Storm surge in Seto Inland Sea with Consideration of the Impacts of Wave Breaking on Surface Currents, *Proceedings of the 32nd International Conference on Coastal Engineering*, ASCE, Shanghai.
- Lee, H. S., T. Yamashita, J. R. C. Hsu, and F. Ding. 2013. Integrated modeling of the dynamic meteorological and sea surface conditions during the passage of Typhoon Morakot, *Dyn. Atmos. Oceans*, 59(0), 1-23.
- Matsumoto, K., T. Takanezawa, and M. Ooe. 2000. Ocean Tide Models Developed by Assimilating TOPEX/POSEIDON Altimeter Data into Hydrodynamical Model: A Global Model and a Regional Model Around Japan, *Journal of Oceanography*, 56, 567-581.
- Miller, L., and B. C. Douglas. 2004. Mass and volume contributions to twentieth-century global sea level rise, *Nature*, 428(6981), 406-409.
- Rahman, A. e. a. 2009. Policy study on the probable impacts of climate change on poverty and economic growth and the options of coping with adverse effect of climate change in Bangladesh, *Rep.*, 117 pp, General Economics Division, Planning Commission, Government of the People's Republic of Bangladesh & UNDP Bangladesh, Dhaka, Bangladesh.
- Rahmstorf, S. 2007. A Semi-Empirical Approach to Projecting Future Sea-Level Rise, *Science*, 315(5810), 368-370.
- Ruane, A. C., et al. 2013. Multi-factor impact analysis of agricultural production in Bangladesh with climate change, *Global Environ. Change*, 23(1), 338-350.
- Sarwar, M. G. M. 2005. Impacts of Sea Level Rise on the Coastal Zone of Bangladesh, M.S. thesis, Lund University International Masters Programme in Environmental Science (LUMES), Lund University, Lund, Sweden.
- Shah, B. V. 1983. Is the environment becoming more hazardous?—A global survey 1947 to 1980, *Disasters*, 7(3), 202-209.
- Tebaldi, C., B. H. Strauss, and C. E. Zervas. 2012. Modelling sea level rise impacts on storm surges along US coasts, *Environmental Research Letters*, 7(1), 014032.
- Trenberth, K. E., et al. 2007. Observations: Surface and Atmospheric Climate Change, in *Climate Change 2007: The Physical Science Basis. Contribution of Working Group I to the Fourth Assessment Report of the Intergovernmental Panel on Climate Change*, edited by S. Solomon, D. Qin, M. Manning, Z. Chen, M. Marquis, K. B. Averyt, M. Tignor and H. L. Miller, pp. 237-336, Cambridge University Press, Cambridge, United Kingdom and New York, NY, USA.
- Tsuge, T., and T. Washida. 2003. Economic valuation of the Seto Inland Sea by using an Internet CV survey, *Marine Pollution Bulletin*, 47(1-6), 230-236.
- Vermeer, M., and S. Rahmstorf. 2009. Global sea level linked to global temperature, *Proceedings of the National Academy of Sciences*, 106(51), 21527-21532.
- Wu, Z., and N. E. Huang. 2009. Ensemble empirical mode decomposition: A noise-assisted data analysis method, *Advances in Adaptive Data Analysis*, 1(1), 1-41.
- Wu, Z., N. E. Huang, S. R. Long, and C.-K. Peng. 2007. On the trend, detrending, and variability of nonlinear and nonstationary time series, *Proceedings of the National Academy of Sciences*, 104(38), 14889-14894.
- Xu, J., and J. S. Long. 2005. Confidence intervals for predicted outcomes in regression models for categorical outcomes, *Stata Journal*, 5(4), 537-559.
- Yamamoto, T. 2003. The Seto Inland Sea—eutrophic or oligotrophic?, *Marine Pollution Bulletin*, 47(1-6), 37-42.
- Yanagi, T., H. Takeoka, and H. Tsukamoto. 1982. Tidal energy balance in the Seto Inland Sea, *Journal of Oceanography*, 38(5), 293-299.